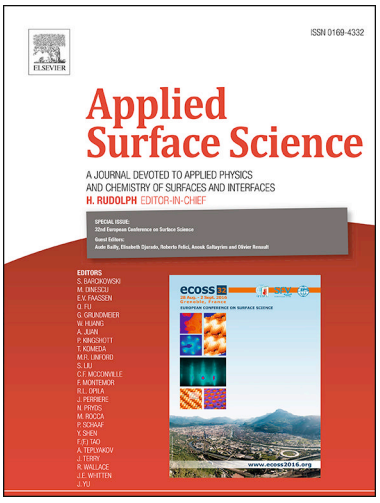

Full Length Article

Controllable crystallinity of nickel oxide film with enhanced electrochromic properties

Shuai Hou, A.I. Gavrilyuk, Jiupeng Zhao, Hongbin Geng, NaLi, Chunxia Hua, Kun Zhang, Yao Li

PII: S0169-4332(18)31179-6
DOI: https://doi.org/10.1016/j.apsusc.2018.04.206
Reference: APSUSC 39205

To appear in: *Applied Surface Science*

Received Date: 29 November 2017
Revised Date: 11 March 2018
Accepted Date: 23 April 2018

Please cite this article as: S. Hou, A.I. Gavrilyuk, J. Zhao, H. Geng, NaLi, C. Hua, K. Zhang, Y. Li, Controllable crystallinity of nickel oxide film with enhanced electrochromic properties, *Applied Surface Science* (2018), doi: https://doi.org/10.1016/j.apsusc.2018.04.206

Controllable crystallinity of nickel oxide film with enhanced electrochromic properties

Shuai Hou[a], A.I. Gavrilyuk[b], Jiupeng Zhao[c], Hongbin Geng[a], NaLi[c], Chunxia Hua[b], Kun Zhang[b], Yao Li*[d]

[a.] School of Materials Science and Engineering, Harbin Institute of technology, Harbin 150001, China.

[b]Ioffe Physical Technical Institute of the Russian Academy of Science,Polytekhnicheskaya 26, Saint-Petersburg, Russia E-mail: gavrilyuk@mail.ioffe.ru

[c.] School of Chemistry and Chemistry Engineering, Harbin Institute of technology, Harbin 150001, China.

[d]Centre for Composite Material, Harbin Institute of technology, Harbin 150001, China. E-mail: yaoli@hit.edu.cn; Fax: +86 451 86402345; Tel: +86 451 86402345

Abstract

A NiO_x film with varying crystallinity across film thickness has been prepared by reactive radio frequency magnetron sputtering. The main research achievement is that the electrochemical cycling stability of the NiO_x film has been radically improved as compared with NiO_x films deposited by the conventional technologies. At the same time, the optical modulation has been also improved, whereas other electrochromic parameters, such as the switching rate and high coloration efficiency have been preserved at the required level.

1. Introduction

Nowadays, a large amount of total energy consumption is expended in the field of commercial and civil buildings throughout the world and electricity is the largest source of

energy for buildings. For the sake of energy saving and emission reduction, the development of new energy efficient materials and technologies is increasingly important. Tremendous research interest is focused in the energy conservation technology used in buildings, such as skylights, roofing, and architecture windows[1-3]. As a promising energy-saving and environmental protection technology, smart windows have been developed due to their capability of switching the optical properties between opaque and transparent states under externally applied voltage [4-7].

Commercial smart windows require the electrochromic (EC) materials with long-term cyclic stability, short switching time and high coloration efficiency (CE). Besides smart windows, EC materials can find application in electronic paper like displays, reusable price labels, military camouflage and spacecraft thermal control [8-16].

There is a variety of electrochromic materials, such as transition metal oxides, conjugated polymers, and mixed valence materials[17-21]. Among them, NiO_x gained a considerable attention due to its good EC properties, low cost, and high coloration efficiency [22-25]. Furthermore, NiO_x can serve as an anodic electrode additionally to a cathodic WO_3 layer in the smart windows, which makes it possible to enhance the transmittance modulation due to joint action of both oxides in the electrochromism[26-30].

However, poor cycling durability severely limits the development of electrochromic NiO_x. When cycling is performed in an aqueous electrolyte under application of an electric field, NiO_x is converted into NiOOH which is easily dissolved in H_2O[31].Therefore, the degradation of NiO_x in aqueous electrolytes is unavoidable. At the same time, the aqueous electrolytes are widely used in the routine research since they give a possibility to compare easily the electrochromic properties

of the NiO_x films prepared by different technologies. It is reported that an exchange of the aqueous electrolytes for anhydrous ones yields the improvement of the cycling stability[32, 33]. However, the reaction between NiO_x and water is not the only the reason for the degradation. Mechanical stresses arising along the coloration/bleaching process can also lead to the film degradation. Both factors can act together and yield the rapid degradation of electrochromic materials during the electrochemical cycling process. Therefore, to minimize the mechanical stresses during the cycling process as well as to improve the mechanical characteristics of the NiO_x films are the main points for the researchers.

As reported before, EC performance and the cristallinity in electrochromic materials are closely connected[22, 34-37]. Polycrystalline electrochromic NiO_x films exhibit low degradation rate by the coloration/decoloration cycling. However, due to a small specific surface area, they demonstrated narrow optical modulation range and low switching speed [38-40].

On the contrary, disordered (quasi-amorphous) films show fast switching speed and large optical modulation range because ions and electrons can easily be inserted /extracted into/from the films having a large specific surface area. Extended defects, such as pores, voids, intergrain boundaries can play the role of channels in surface diffusion for various ions. These “channels” are filled with an electrolyte and ions easily move along the natural pathways. On the other hand, the easy surface diffusion and small grains in the disordered films predetermine the possibility for the ions to find the easiest way for intercalation /extraction into/out the grains from different crystallographic directions. But the cycling stability of these films is low; they demonstrate a high degradation rate, which is the

deterioration of the electrochromic performances during coloration/bleaching cycles [22, 39, 41]. Therefore, the aim of our research was to create a NiO_x structure that combines positive features of both crystalline and quasi amorphous films and can essentially enhance electrochromic performances of the NiO_x films.

In this research, the NiO_x film with varying crystallinity, changing from highly ordered (in the domains close to the transparent electrode) to highly disordered (at the film surface) across the film thickness was deposited onto an ITO coated glass substrate by the reactive radio frequency magnetron sputtering. The NiO_x film with the varying degree of crystallinity was prepared by varying the substrate temperature (T_s) during the sputtering process. The tests showed that this film has the enhanced EC characteristics including fast switching speed, high CE, large optical modulation range and good cycling durability.

2. Experimental

2.1. Preparation of the films by conventional technologies

The NiO_x films were deposited in O_2 (99.99% purity) and Ar (99.99% purity) gas mixture by reactive radio frequency (RF) magnetron sputtering technology using metallic Ni (99.99% purity) of 5 cm diameter as a target. Indium tin oxide coated (ITO or SnO_2:In) (1 cm × 4 cm in size, sheet resistance R_s= 8Ωsquare^{-1} glasses washed for 10 min with acetone, ethanol, and de-ionized water in an ultrasonic bath were used as substrates. The distance between the target and the substrate was 100 mm. During the deposition process, O_2/Ar mass flow ratio of 1 was maintained by a working pressure of 3 Pa and the RF power of 50 W.

We prepared a series of the NiO_x films of same thickness deposited at different T_s ranging from 25^0C to 350^0C. Their electrochromic characteristics were tested in order to compare with those of the film prepared by the new technology.

2.2 Preparation of the films with variable crystallinity across the film thickness

The main idea of our work was to change the crystallinity in the NiO_x film during the deposition. The spirit of the research was to manufacture the film that combines the positive features of the highly ordered and highly disordered films and providing very gradual changes in the film structure along film thickness.

At the beginning of the deposition, T_s was maintained at 350°C for 2 minutes in order to provide the formation of the highly ordered polycrystalline NiO_x layer. After that, the substrate heater was switched off, T_s was continuously and gradually decreasing, and the crystallinity of the subsequently deposited layers continuously was becoming lower. Finally, the deposition process was stopped when T_s lowered down to 80°C and the crystallinity of the NiO_x film outermost layers at the film surface was worst. As in the previous case, film thickness measured by SEM has a value of about 200 nm, whereas thickness of the layer deposited at 350^oC was about 20 nm.

The scheme of the crystalliniy gradient in the NiO-DG film is demonstrated in Fig. 1 (a) and the photos of NiO-DG in the bleached state (transparent) and the colored state (brown) are shown in Fig. 1 (b) and (c), respectively.

2.3 Methods of characterization of the films

The structure of the deposited NiO_x films was identified by a glancing angel X-ray diffractometer (GAXRD, Panalytical) using a Cu-K_α (λ=0.154 nm) radiation source.

The film surface morphology was investigated by a scanning electron microscope (SEM, Helious Nanolab 600j) and Atomic Force Microscope (AFM, Dimension Fast Scan^{TM}).Film thickness measured by SEM has a value of about 200 nm.

The film electrochromic properties were investigated by cyclicvoltammetry (CV) and chronoamperometry (CA), which were conducted by CHI 660C electrochemical workstation (Shanghai Chen Hua Instrument Co. Ltd.).A three-electrode cell was used consisting of working electrode (the NiO film on an ITO substrate), a counter electrode (platinum foil of an area=2×4 cm^2), and a reference electrode (Hg/HgO) plunged into a 1.0 M KOH electrolyte.

To provide a synchronous operation of the light source and the spectrometer by the registration of the NiO_x film transmission spectra in the range from 380 to 800 nm the special device developed in our group was used. Films illumination was carried out from a light source(DT-mini-2-GS, Ocean Optics) through an optical fiber; an optical spectrometer MAYA 2000-Pro, (Ocean Optics) was used to register the spectra.

3. Results and discussion

The NiO_x film with the varying crystallinity is denoted as NiO-DG, whereas the films deposited at T_s between 25 up to 350 ℃ are denoted as NiO-25, NiO-100, NiO-200, NiO-300, and NiO-350, respectively.

XRD measurements were carried out to discover the influence of T_s on the crystallinity of the NiO_x films. The XRD patterns for the samples prepared under different conditions are shown in Fig.2. No Bragg diffraction peaks, except those from the ITO, were observed in NiO-25 and NiO-100 films which demonstrate a high degree of disorder. With the increase

of T_s, the crystallinity of the NiO_x films was noticeably improved. Crystallization of NiO_x occurs between 100 and 200 ℃, results in the change of the XRD patterns. According to the Joint Committee on Powder Diffraction Standards (JCPDS) cards No. 89-7130 and No. 89-4597, NiO_x has a cubic structure with the diffraction peaks from (111) and (200) planes. When the T_s reached 200 ℃, the characteristic peak at 42.90 appears, which can be assigned to a (200) reflex of NiO_x. The peak intensity was significantly enhanced withthe increase in T_s (Fig.1).XRD pattern of NiO-DG is similar to that of NiO-350 and NiO-300 and characteristic peaks of NiO_x can be detected in that sample which can be ascribed to the crystalline part at the bottom side.

The atomic force images of the NiO_x film surface deposited at various T_s are shown in Fig.3 and Fig.4 which present two dimensional and three dimensional images, respectively. The surface roughness was determined in tapping mode; the values of the mean roughness (R_a) and the root mean square roughness (R_q) are presented in Fig.5. For comparison, two-dimensional and three-dimensional AFM images for ITO substrate are presented in Fig. S1. The values of R_a and R_q for ITO substrate are 0.25 and 0.38.

One can compare Fig.3 (a) and 3(e), which show that the grain size in NiO-25 is much smaller than that in NiO-350 and the NiO-25 surface is much rougher than that in other samples, especially as compared with that in NiO-350. Fig. 5 shows that the values of R_a and R_q are the highest in the NiO_x films deposited at 25℃ and continuously decrease with the increase in T_s unless getting the minimal values at T_s=350^{0}C. Two dimensional and three dimensional images of NiO-DG are presented in Fig.3 (f) and 4(f) and the corresponding value of R_a and R_q are 4.67 and 3.84. These values are higher than the samples prepared at substrate temperatures above 100 ℃

which means the surface morphology of NiO-DG is much rougher than most of other samples. It is obvious that there is a strong dependence between surface morphology and the EC performance since the film surface contacts an electrolyte and the specific surface area determines the concentration of electrochemically active reaction sites[42]. As it was mentioned above, the pores, voids, and intergrain boundaries can serve as channels for easy diffusion of ions inserted and extracted by the electrochromism. The films with rougher surface morphology have a larger specific surface area and a more developed surface, which makes them more effective in providing of the insertion/extraction of guest ions[34, 42]. For comparison, the SEM imagines are presented in Fig. S2 in the supporting information.

Current-voltammetry (CV) measurements were performed in order to investigate the electrochemical properties of the NiO_x films. Fig. 6(a) presents the CV curves for the films deposited under different conditions. The curves were registered at a scan rate of 50 mV s^{-1} with the use of a 1.0 M KOH electrolyte within a potential range between 0 and to 0.7 V. For all the samples, the CV dependences exhibit the oxidation and reduction peaks associated with the coloration and bleaching, correspondingly (Fig.6). The coloration process of the films corresponds to the oxidation peak and the bleaching process is associated with the reduction peak, which can be attributed to the following electrochemical reaction:

$$Ni(OH)_2 \text{ (bleached)} + OH^- \longleftrightarrow NiOOH \text{ (colored)} + H_2O + e^- \quad (1)$$

The insertion and extraction of OH^- ions leads to the appearance and disappearance of the non-isovalent Ni states which causes coloration/decoloration.

The amount of charge inserted and extracted during the electrochromic process is calculated by

the following equations:

$$Q = \int Idt \tag{2}$$

$$v = \frac{dV}{dt} \tag{3}$$

Where Q, I, v and V are: amount of charge, instantaneous current, scan rate of the CV curves, and instantaneous potential, correspondingly. From the equation (2) and (3), Q can be obtained as:

$$Q = \frac{\int IdV}{v} \tag{4}$$

Fig.6 (b) demonstrates the charge densities during the insertion and extraction process for the films prepared at different T_s. With the increase in T_s, both amounts of inserted and extracted charge decrease significantly. The specific data was demonstrated in Table S1 in the supporting information. The total inserted and extracted charge in NiO-25 is much larger than in the other samples, which is attributed to its disorder and a great specific surface[43]. Besides, the total inserted and extracted charge in NiO-DG are 4.4523 mC/cm^2 and 3.4622 mC/cm^2 which are not presented in Fig. 6 (b) but shown in Table S1. From Fig. 6 (a) we can also clearly see that the CV area of NiO-25 and NiO-DG is much larger than the other samples.

CA tests provided along with the in-situ transmission spectra measurements were performed in NiO_x-DG using 1.0 M KOH. Fig.7 (a) presents the transmission spectra in the colored and bleached states in the range from 380 nm to 800 nm. NiO-DG exhibits a pronounced electrochromism already in the initial stage of the cycling and the modulation of the transmittance in NiO-DG is enhanced after 1000 cycles (Fig.8), which can be attributed to the “activation” of NiO-DG film. According to, it is possible that ion intercalation is promoted by opening up of the initially compact layers of NiO-DG rendering the structure more inclined to easy diffusion. At this stage, the morphology of the as-prepared films is progressively modified by the continuous

injection/ extraction of charge carriers.

The switching speed is one of the most important parameters in EC performance. The in situ transmittance measurements at 550 nm were provided to investigate the switching parameters of the NiO-DG films. The response times are defined as the duration to reach 90% of its full modulation at a particular wavelength. The NiO-DG exhibits both short coloration and bleaching times 3.1 s and 2.1 s, correspondingly, as shows Fig.7 (b) and, which close to the data previously reported[25, 44-46]. The amazingly reproducible transmittance curves demonstrated in Fig. 7(c) were registered synchronous to the CA measurements, which demonstrate an excellent electrochromic performance of NiO-DG.

The coloration efficiency (CE) is a key parameter in comparison between different electrochromic materials. It is determined as the optical density change (ΔOD) per unit of charge (Q) inserted/extracted into/from an EC film:

$$CE(\lambda) = \frac{\Delta OD(\lambda)}{Q} \tag{6}$$

$$\Delta OD(\lambda) = \log\frac{T_b}{T_c} \tag{7}$$

$$Q = \int_{t_2}^{t_1} j(t)dt \tag{8}$$

Where T_b and T_c are the values of the film transmittance for the bleached and colored states, correspondingly; Q is the value of the inserted (or extracted) charge during the coloration period. A high value of CE indicates that the EC material shows a large modulation range of the transmittance achieved by a small value of the inserted charge[47]. Using the equations above, we calculated CE for NiO-DG, which is 51.6 cm^2C^{-1}. This value lies within the range of the data previously reported in many papers on electrochromism in NiO_x [15, 48]. The high CE results

from the high degree of disorder in the film surface layers, which provides the diffusion along the grain boundaries[35, 49].

The cycling stability in electrochromic materials plays a critically important role for practical applications. Herein, the durability tests were performed by CA measurements in a parallel run with the in-situ transmittance spectra measurements for NiO-25, NiO-350 and NiO-DG at the wavelength of 550 nm. The results are presented in Fig. 8, whereas several important EC parameters are collected in Table 1.

At the initial stage of cycling, the optical modulation in NiO-25 is the largest as compared with NiO-350 and NiO-DG (see Table 1), which can be attributed to its disorder and high specific surface area. At the same time, the electrochemical cycling leads to rapid degradation of the electrochromic performance. After a period of initial instability, the EC performance then declines dramatically after 270 cycles and the transmittance fluctuates at the bleached state (T_b) violently after 300 cycles, as shows Fig. 8(a). At the end of cycling, T_b of NiO-25 decreased to about 25.6% compared with 55.6% at the beginning of the cycling.

As compared with NiO-25, the crystalline quality of NiO-350 is much higher. The compact structure impedes insertion/extraction of ions into/from the film and, as a result of that, the optical modulation range decayed fast from 55.63% to 35.0%, as shown in Table.1. At the same time, due to the better crystallinity, the cycling durability in NiO-350 is much higher. Figure 8 (c) illustrates the transmittance variation of NiO-350 in the course of 1000 cycles. In the first 500 cycles, T_b can be maintained at a level ~ 90% and the optical modulation range is gradually getting larger. Unfortunately, further cycling yields a decay in the both T_b and T_c down to 63.02% and 12.12%, correspondingly, after 1000 cycles, see Fig. 8(d).

In NiO-DG, the electrochromic performance can be significantly improved. As demonstrated in Fig. 8(e), after a short increase at the initial stage of cycling, T_b of NiO-DL persists at about 90% during the further process. In the meantime, T_c gradually decreases from 56.9% to 22.7% with the cycling. Finally, the optical modulation range at 550 nm was enhanced to about 67.6% after 1000 cycles. In addition, the response time is much shorter than that in NiO-350, as displayed in Table 1, which can be attributed to the unique structure of the NiO-DG. The crystallinity in NiO-DG is reduced smoothly along the film thickness from the ITO electrode to the film surface, which provides easy ion diffusion along the intergrain boundaries, whereas the most ordered domains resist to degradation. Eventually, the EC performance of NiO-DG could be improved on the basis of its unique crystal structure.

The results obtained can be understood within the frames of the idea expressed by Granqvist who claimed that the diffusion is hampered in the initially disordered films, whereas the compact films become open up to easy diffusion under cycling. It is possible to observe that NiO-25 films lose their efficiency already after 250 cycles.

NiO-350 films behave differently. One can see that the modulation range is enhanced during first 500 cycles due to opening up of its compact structure.

NiO-DG films demonstrated the best cycling stability, which is confirmed by Fig.8(f). One can notice that there is no sign of the degradation after 1000 cycles, which is the best result among all technologies considered. Besides this, the modulation of the transmittance by electrochemical cycling was noticeably enhanced.

4. Conclusions

Using the radio frequency magnetron sputtering we prepared electrochromic NiO_x films with continuous variation in crystallinity from highly ordered, close to the transparent ITO electrode, to highly disordered at the film surface. The changes in the film crystallinity were provided by a continuous decrease in T_s along the sputtering process.

The film combined fast operation times, which is usually inherent to the highly disordered NiO_x films with a great specific surface area, and enhanced resistance to the film degradation during the electrochromic cycling, which can be attributed to a lower value of mechanical stresses arising in the film upon insertion/extraction of ions.

Therefore, the achievement of this research is the creation of the film structure which possesses the EC parameter inherent to the highly disordered films, such as low coloration and bleaching times and high coloration efficiency and, at the same time, radically enhances the most important parameter for practical applications of electrochromism, such as the cycling stability.

Acknowledgements

We thank National Natural Science Foundation of China (No.51572058, 51502057), the International Science & Technology Cooperation Program of China (2013DFR10630, 2015DFE52770), National Key Research & Development Program (2016YFB0303903), and the Foundation of Science and Technology on Advanced Composites in Special Environment Laboratory.

References

[1] M.G. Debije, Solar Energy Collectors with Tunable Transmission, Advanced Functional Materials, 20 (2010) 1498-1502.

[2] L.P.L. M. P. Gutierrez, Multiscale design and integration of sustainable building functions, Science, 341 (2013) 247-248.

[3] M.P. Gutierrez, T.I. Zohdi, Effective reflectivity and heat generation in sucrose and PMMA mixtures, Energy and Buildings, 71 (2014) 95-103.

[4] C.-G. Granqvist, Electrochromic materials: Out of a niche, Nat Mater, 5 (2006) 89-90.

[5] V.K. Thakur, G. Ding, J. Ma, P.S. Lee, X. Lu, Hybrid materials and polymer electrolytes for electrochromic device applications, Advanced materials, 24 (2012) 4071-4096.

[6] C.G. Granqvist, Electrochromic devices, Journal of the European Ceramic Society, 25 (2005) 2907-2912.

[7] C. Yan, W. Kang, J. Wang, M. Cui, X. Wang, C.Y. Foo, K.J. Chee, P.S. Lee, Stretchable and Wearable Electrochromic Devices, ACS Nano, 8 (2014) 316-322.

[8] C. Costa, C. Pinheiro, I. Henriques, C.A. Laia, Inkjet printing of sol-gel synthesized hydrated tungsten oxide nanoparticles for flexible electrochromic devices, ACS applied materials & interfaces, 4 (2012) 1330-1340.

[9] F. Lin, D. Nordlund, T.-C. Weng, R.G. Moore, D.T. Gillaspie, A.C. Dillon, R.M. Richards, C. Engtrakul, Hole Doping in Al-Containing Nickel Oxide Materials To Improve Electrochromic Performance, ACS applied materials & interfaces, 5 (2013) 301-309.

[10] H. Li, G. Shi, H. Wang, Q. Zhang, Y. Li, Self-seeded growth of nest-like hydrated tungsten trioxide film directly on FTO substrate for highly enhanced electrochromic performance, Journal of Materials Chemistry A, 2 (2014) 11305.

[11] D.R. Rosseinsky, R.J. Mortimer, Electrochromic Systems and the Prospects for Devices, Advanced materials, 13 (2001) 783-793.

[12] R.J. Mortimer, A.L. Dyer, J.R. Reynolds, Electrochromic organic and polymeric materials for display applications, Displays, 27 (2006) 2-18.

[13] Z. Xie, X. Jin, G. Chen, J. Xu, D. Chen, G. Shen, Integrated smart electrochromic windows for energy saving and storage applications, Chemical communications, 50 (2014) 608-610.

[14] D.D. Yao, R.A. Rani, A.P. O'Mullane, K. Kalantar-zadeh, J.Z. Ou, High Performance Electrochromic Devices Based on Anodized Nanoporous Nb2O5, The Journal of Physical Chemistry C, 118 (2014) 476-481.

[15] J.-h. Zhang, J.-p. Tu, D. Zhou, H. Tang, L. Li, X.-l. Wang, C.-d. Gu, Hierarchical SnO2@NiO core/shell nanoflake arrays as energy-saving electrochromic materials, J. Mater. Chem. C, 2 (2014) 10409-10417.

[16] P.M.B. Robert A Colley, John R Owen and Simon Balderson, Poly[oxymethylene–oligo(oxyethylene)] for use in subambient temperature electrochromic devices, Polym. Int., 49 (2000) 371-376.

[17] G.J. Stec, A. Lauchner, Y. Cui, P. Nordlander, N.J. Halas, Multicolor Electrochromic Devices Based on Molecular Plasmonics, ACS Nano, (2017).

[18] X. Xia, D. Chao, X. Qi, Q. Xiong, Y. Zhang, J. Tu, H. Zhang, H.J. Fan, Controllable growth of conducting polymers shell for constructing high-quality organic/inorganic core/shell nanostructures and their optical-electrochemical properties, Nano Lett, 13 (2013) 4562-4568.

[19] M.L. Moser, G. Li, M. Chen, E. Bekyarova, M.E. Itkis, R.C. Haddon, Fast Electrochromic Device Based on Single-Walled Carbon Nanotube Thin Films, Nano Lett, 16 (2016) 5386-5393.

[20] X. Xia, Z. Ku, D. Zhou, Y. Zhong, Y. Zhang, Y. Wang, M.J. Huang, J. Tu, H.J. Fan, Perovskite solar cell powered electrochromic batteries for smart windows, Mater. Horiz., 3 (2016) 588-595.

[21] M.-S. Fan, S.-Y. Kao, T.-H. Chang, R. Vittal, K.-C. Ho, A high contrast solid-state electrochromic device based on nano-structural Prussian blue and poly(butyl viologen) thin films, Solar Energy Materials and Solar Cells, 145 (2016) 35-41.

[22] K. Zhou, Z. Qi, B. Zhao, S. Lu, H. Wang, J. Liu, H. Yan, The influence of crystallinity on the electrochromic properties and durability of NiO thin films, Surfaces and Interfaces, 6 (2017) 91-97.

[23] G. Cai, P. Darmawan, M. Cui, J. Chen, X. Wang, A.L. Eh, S. Magdassi, P.S. Lee, Inkjet-printed all solid-state electrochromic devices based on NiO/WO3 nanoparticle complementary electrodes, Nanoscale, 8 (2016) 348-357.

[24] M. Da Rocha, A. Rougier, Electrochromism of non-stoichiometric NiO thin film: as single layer and in full device, Applied Physics A, 122 (2016).

[25] D.S. Dalavi, R.S. Devan, R.S. Patil, Y.-R. Ma, M.-G. Kang, J.-H. Kim, P.S. Patil, Electrochromic properties of dandelion flower like nickel oxide thin films, J. Mater. Chem. A, 1 (2013) 1035-1039.

[26] M. P. Browne, Electrochromic Nickel Oxide Films for Smart Window Applications, International Journal of Electrochemical Science, (2016) 6636-6647.

[27] Y. Zhou, X. Diao, G. Dong, Z. Wu, D. Dong, M. Wang, Enhanced transmittance modulation of ITO/NiO x /ZrO2:H/WO3/ITO electrochromic devices, Ionics, 22 (2015) 25-32.

[28] K.K. Chiang, J.J. Wu, Fuel-assisted solution route to nanostructured nickel oxide films for electrochromic device application, ACS applied materials & interfaces, 5 (2013) 6502-6507.

[29] X.H. Xia, J.P. Tu, J. Zhang, X.L. Wang, W.K. Zhang, H. Huang, Electrochromic properties of porous NiO thin films prepared by a chemical bath deposition, Solar Energy Materials and Solar Cells, 92 (2008) 628-633.

[30] C.G. Granqvist, Solar Energy Materials, Adv. Mater, 15 (2003).

[31] Y.-T.P.a.K.-T. Lee, Degradation mechanism of the complementary electrochromic devices with WO3 and NiO thin films fabricated by RF sputtering deposition, Journal of Ceramic Processing Research, 17 (2016) 1192~1196.

[32] Q. Liu, G. Dong, Y. Xiao, M.-P. Delplancke-Ogletree, F. Reniers, X. Diao, Electrolytes-relevant cyclic durability of nickel oxide thin films as an ion-storage layer in an all-solid-state complementary electrochromic device, Solar Energy Materials and Solar Cells, 157 (2016) 844-852.

[33] R.-T. Wen, G.A. Niklasson, C.G. Granqvist, Electrochromic nickel oxide films and their compatibility with potassium hydroxide and lithium perchlorate in propylene carbonate: Optical, electrochemical and stress-related properties, Thin Solid Films, 565 (2014) 128-135.

[34] B.X.F. S.R. Jiang , P.X. Yan, X.M. Cai, S.Y. Lu. , The effect of annealing on the electrochromic properties of microcrystalline NiOx films prepared by reactive magnetron rf sputtering, Applied Surface Science, 174 (2001) 125-131.

[35] K.K. Purushothaman, G. Muralidharan, The effect of annealing temperature on the electrochromic properties of nanostructured NiO films, Solar Energy Materials and Solar Cells, 93 (2009) 1195-1201.

[36] H. Zheng, J.Z. Ou, M.S. Strano, R.B. Kaner, A. Mitchell, K. Kalantar-zadeh, Nanostructured Tungsten Oxide - Properties, Synthesis, and Applications, Advanced Functional Materials, 21 (2011) 2175-2196.

[37] S.B. Sallard, T. Smarsly, B. M., Electrochromic Stability of WO3 Thin Films with Nanometer-Scale Periodicity and Varying Degrees of Crystallinity, J. Phys. Chem. C, 111 (2007) 7200-7206.

[38] T. Maruyama, S. Arai, The electrochromic properties of nickel oxide thin films prepared by chemical vapor deposition, Solar Energy Materials and Solar Cells, 30 (1993) 257-262.

[39] K. Zhou, H. Wang, Y. Zhang, J. Liu, H. Yan, An Advanced Technique to Evaluate the Electrochromic Performances of NiO Films by Multi-Cycle Double-Step Potential Chronocoulometry, Journal of The Electrochemical Society, 163 (2016) H1033-H1040.

[40] M. Deepa, A.K. Srivastava, K.N. Sood, S.A. Agnihotry, Nanostructured mesoporous tungsten oxide films with fast kinetics for electrochromic smart windows, Nanotechnology, 17 (2006) 2625.

[41] G.A. Niklasson, C.G. Granqvist, Electrochromics for smart windows: thin films of tungsten oxide and nickel oxide, and devices based on these, J. Mater. Chem., 17 (2007) 127-156.

[42] P.X.Y. S.R. Jiang, B.X. Feng, X.M. Cai, J. Wang, The response of a NiOx thin film to a step potential and its electrochromic mechanism, Materials Chemistry and Physics, 77 (2002) 384-389.

[43] S.H. Lee, R. Deshpande, P.A. Parilla, K.M. Jones, B. To, A.H. Mahan, A.C. Dillon, Crystalline WO3 Nanoparticles for Highly Improved Electrochromic Applications, Advanced materials, 18 (2006) 763-766.

[44] Z. Chen, A. Xiao, Y. Chen, C. Zuo, S. Zhou, L. Li, Highly porous nickel oxide thin films prepared by a hydrothermal synthesis method for electrochromic application, Journal of Physics and Chemistry of Solids, 74 (2013) 1522-1526.

[45] Y.F. Yuan, X.H. Xia, J.B. Wu, Y.B. Chen, J.L. Yang, S.Y. Guo, Enhanced electrochromic properties of ordered porous nickel oxide thin film prepared by self-assembled colloidal crystal template-assisted electrodeposition, Electrochimica Acta, 56 (2011) 1208-1212.

[46] J. Liu, Y. Ren, B. Dasgupta, H. Tanoto, H.L. Seng, W.K. Chim, S.F.Y. Li, S.Y. Chiam, The role of ions and reaction sites for electrochemical reversible charge cycling in mesoporous nickel hydroxides, Journal of Materials Chemistry A, 1 (2013) 15095.

[47] M.R. Scherer, U. Steiner, Efficient electrochromic devices made from 3D nanotubular gyroid networks, Nano Lett, 13 (2013) 3005-3010.

[48] J.-h. Zhang, G.-f. Cai, D. Zhou, H. Tang, X.-l. Wang, C.-d. Gu, J.-p. Tu, Co-doped NiO nanoflake array films with enhanced electrochromic properties, Journal of Materials Chemistry C, 2 (2014) 7013.

[49] X.C. Lou, X.J. Zhao, Y.L. Xiong, X.T. Sui, The influence of annealing on electrochromic properties of Al–B–NiO thin films prepared by sol–gel, Journal of Sol-Gel Science and Technology, 54 (2010) 43-48.

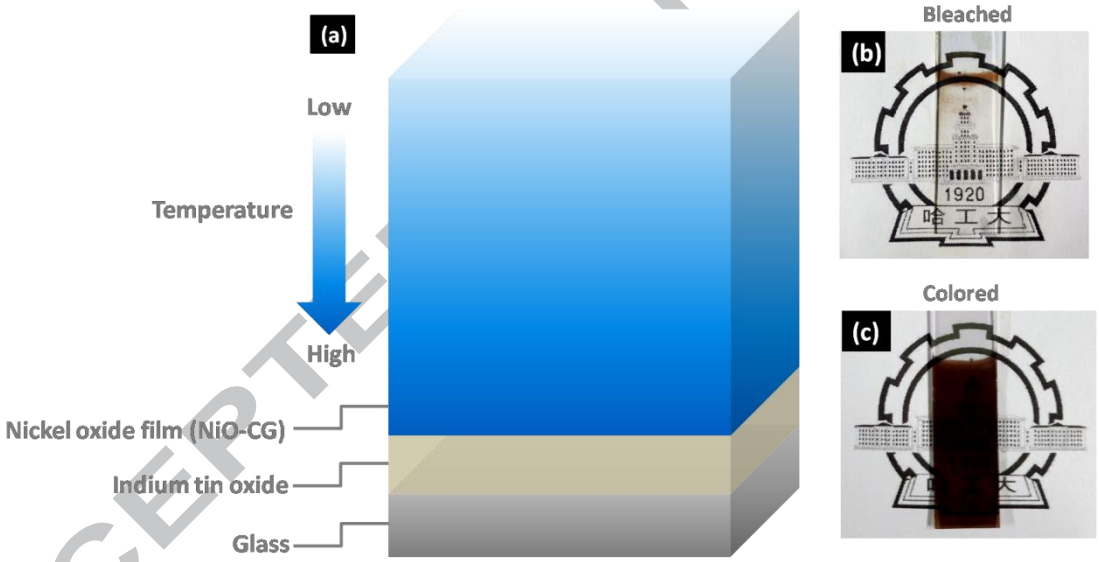

Fig. 1 (a) Schematic of the crystallinity gradient in NiO_x film (NiO-DG) and photos of NiO-DG in the bleached state (b) and in the colored state (c). The deeper is the blue color– the better the crystallinity.

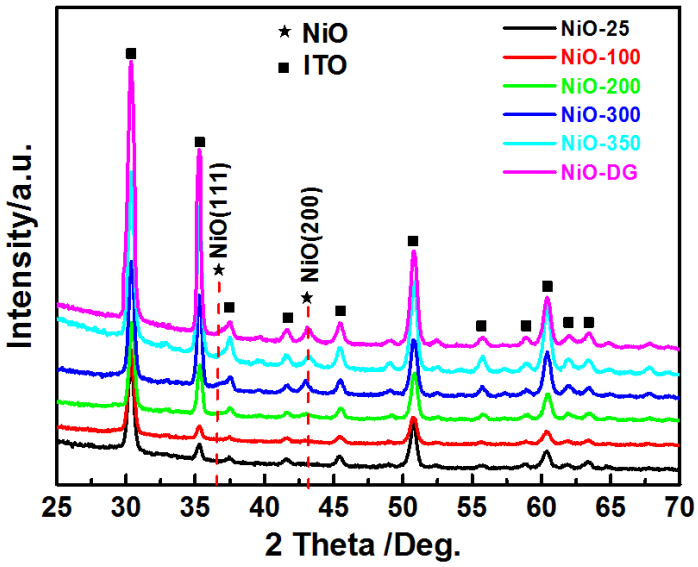

Fig. 2 XRD patterns of NiO_x films prepared at different conditions.

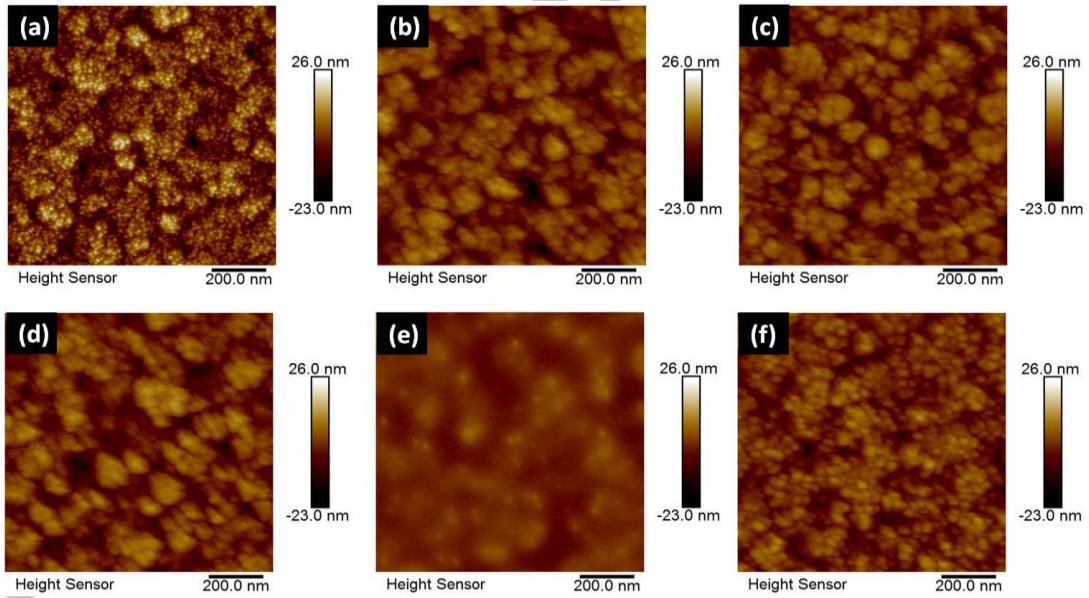

Fig. 3 Two-dimensional AFM images for NiO-25 (a), NiO-100 (b), NiO-200 (c), NiO-300 (d) NiO-350 (e) and NiO-DG (f).

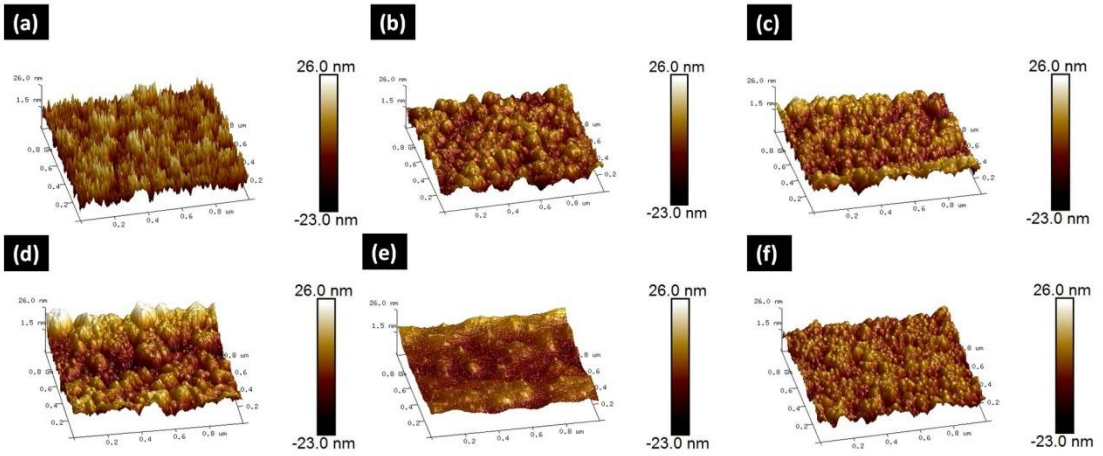

Fig. 4 Three-dimensional AFM images for NiO-25 (a), NiO-100 (b), NiO-200 (c), NiO-300 (d),NiO-350 (e) and NiO-DG (f).

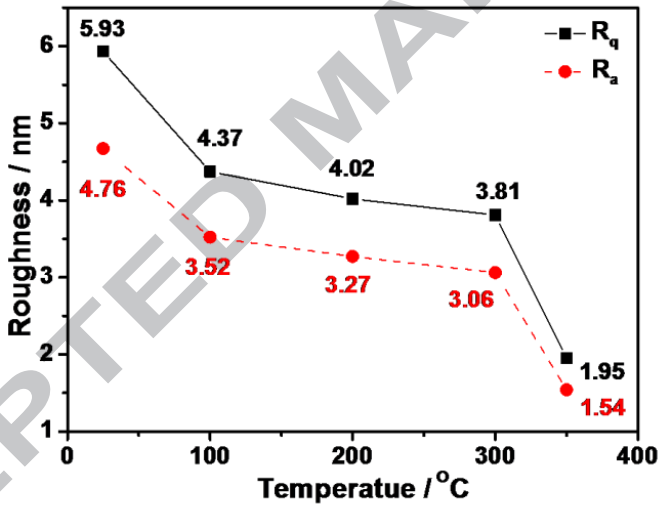

Fig. 5 Mean surface roughness (R_a) and root mean square roughness (R_q) of nickel oxide films deposited at various substrate temperatures.

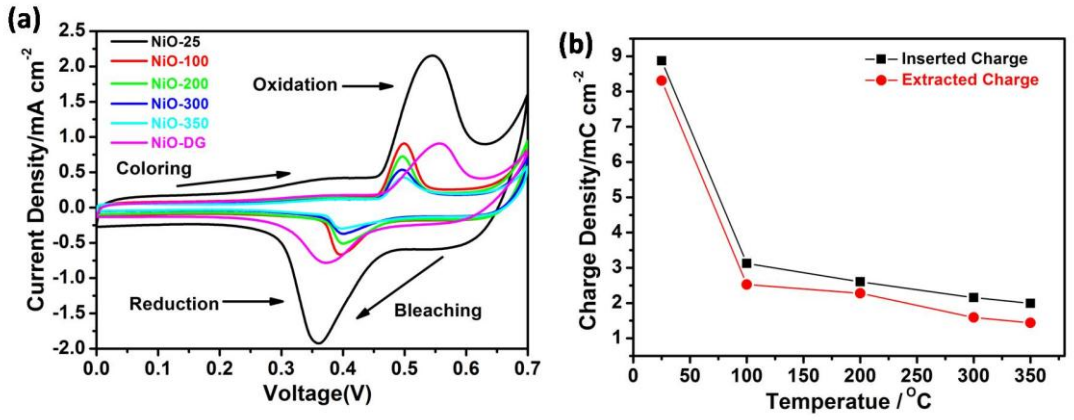

Fig. 6 (a) C-V dependences for NiO_x thin films prepared at different conditions in the potential range between 0 and 0.7 V at the scan rate of 50 mV s^{-1} (b) Densities of the inserted and extracted charge for NiO_x thin films prepared at different substrate temperature determined from CV data.

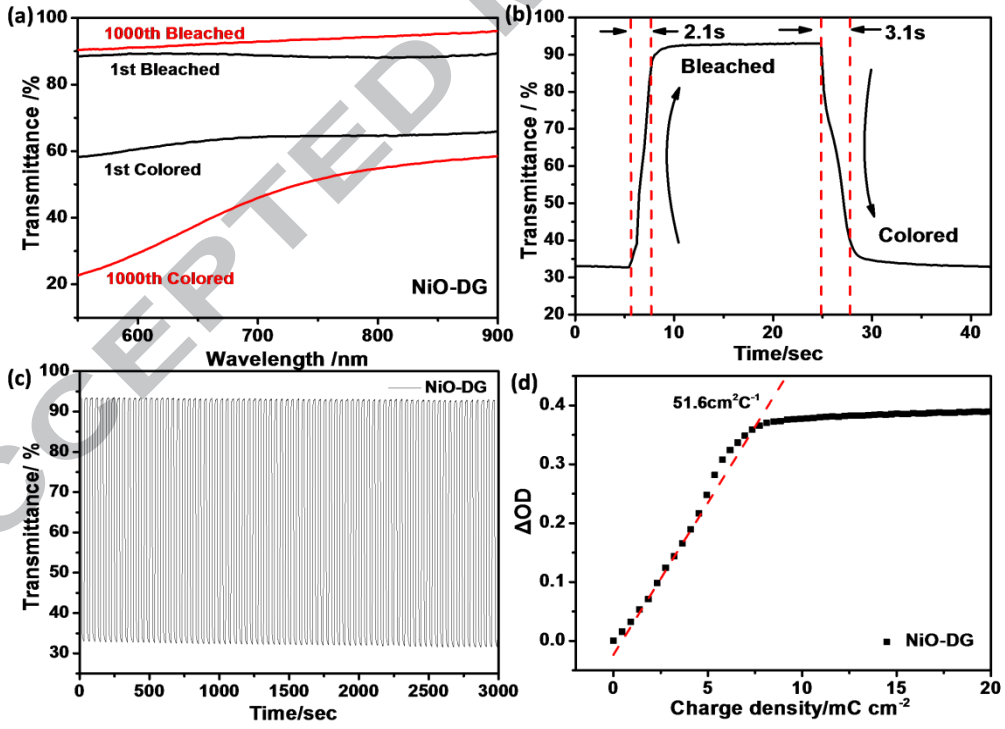

Fig. 7 (a) Transmittance spectra of the colored and bleached states for the NiO-DG film in the range between 350 up to 800 nm for the first and for 1000th cycle. (b) One single coloration–bleaching cycle displays the switching response characteristics. (c) 75

coloration–bleaching cycles at 550 nm. (d) The variation of the optical density (OD) was measured in situ versus the charge density.

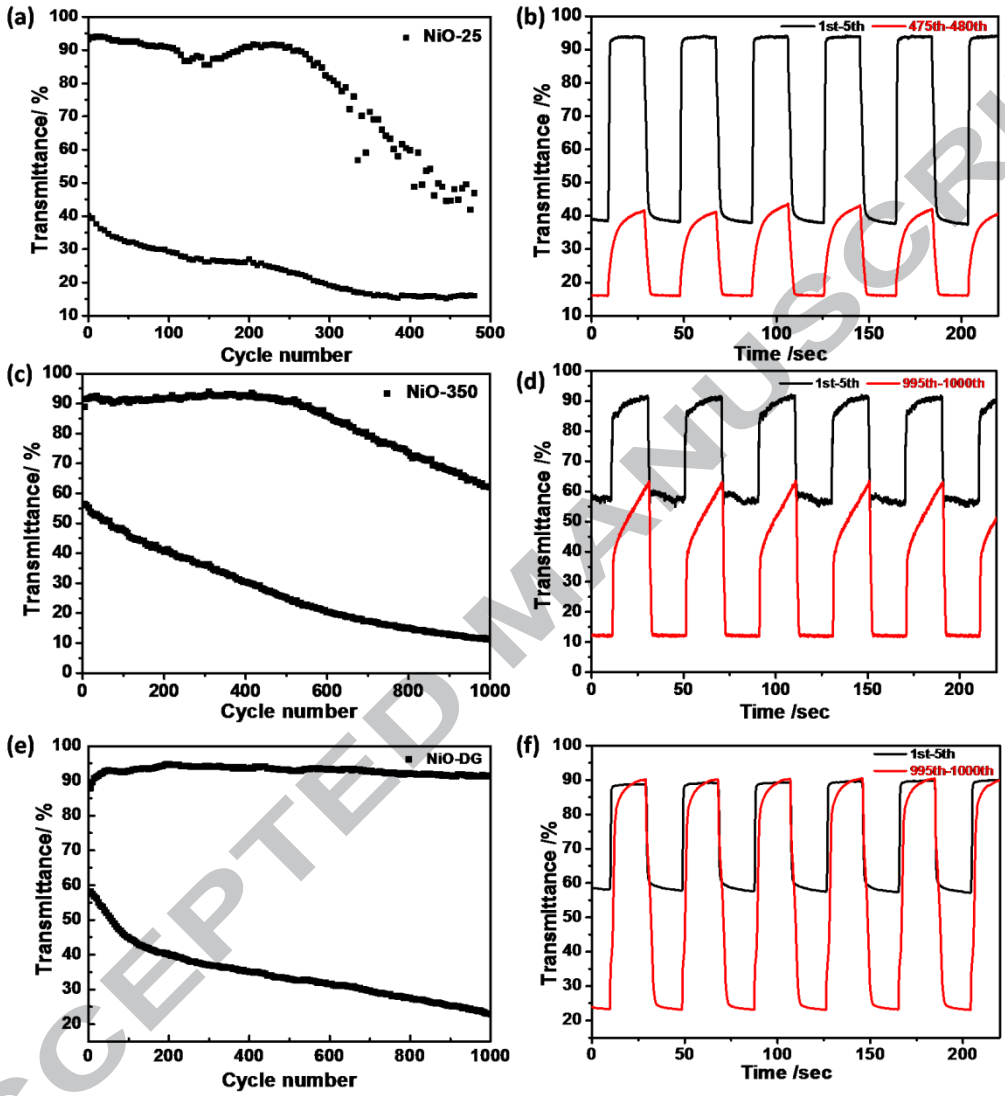

Fig. 8 Durability tests of NiO-25 (a), NiO-300 (c) and NiO-DG (e) at wavelength of 550 nm. In-situ transmittance of NiO-25 (b), NiO-300 (d) and NiO-DG (f) for the first five cycles and the last five cycles.

Table 1. Comparison of the EC performances for NiO-25, NiO-300 and NiO-DG

Samples	1st - 5th					995th - 1000th				
	T_b(%)	T_c(%)	ΔT(%)	t_b(s)	t_c(s)	T_b(%)	T_c(%)	ΔT(%)	t_b(s)	t_c(s)
NiO-25	93.6	38.0	55.6	0.8						
NiO-350	91.7	56.7	35.0	4.3	7.62	63.0	12.1	50.9	16.1	1.5
NiO-DG	89.8	56.9	32.9	0.9	2.82	90.3	22.7	67.6	4.3	4.3

Graphical abstract

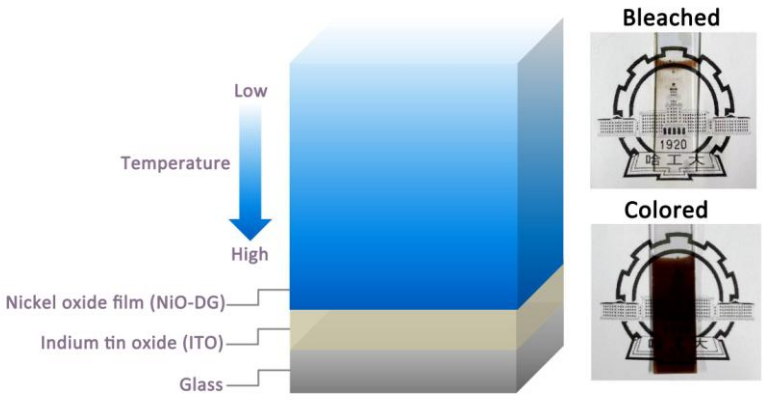

Highlights

1. We prepared a NiO_x electrochromic film with the crystallinity varying across film thickness for the first time.
2. We provided a series of tests measuring electrochromic parameters of the prepared film.
3. The film with variable crystallinity showed an enhanced cycling durability as compared with the NiO_x film prepared by conventional technologies.